Dynamic causal modeling computational pipeline for resting-state fMRI data: the structure and main modules for DCM and PEB analysis

A. N. Silchenko[1], E. Betazzi[1,2], S.B. Eickhoff[1,2], M. Tahmasian[1,2], F. Hoffstaedter[1,2]

[1]Institute of Neuroscience and Medicine (INM-7: Brain and Behaviour), Research Centre Jülich, Jülich, Germany;
[2]Institute of Systems Neuroscience, Heinrich Heine University Düsseldorf, Düsseldorf, Germany
a.silchenko@fz-juelich.de

Introduction

- Resting-state functional magnetic resonance imaging (fMRI) is a standard tool used to investigate brain network connectivity. Most studies characterizing the intrinsic organization of resting-state networks are based on functional connectivity (FC), which cannot capture the directionality of observed interactions. A dynamic causal modelling (DCM) approach can be applied to infer causal influences between regions [1].
- We developed a computational pipeline to analyze the effective connectivity (EC) of the resting-state fMRI data. The original input resting-state fMRI data are assumed to be in standard BIDS/FMRIPREP format [2]. It is also assumed that the analyzed network comprises a set of regions of interest (ROIs) which can be defined using either a brain atlas or spheres around the chosen coordinates [3].
- EC analysis is performed using spectral DCM for the BOLD signals, which were extracted from the predefined ROIs as a result of singular value decomposition [4]. The values of the connectivity parameters computed for a set of the most probable models form the primary output of the DCM pipeline. Parametric Empirical Bayesian (PEB) and Bayesian Model Reduction (BMR) approaches are used to reveal the best model at the group level [5,6].

DCM framework

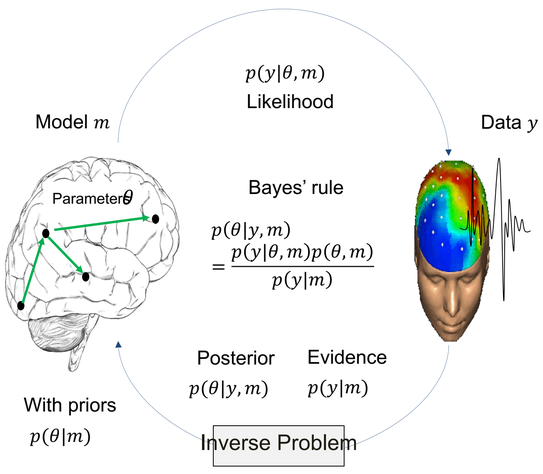

Model Specification, Inversion and Comparison / Averaging

1. Hypotheses are formulated as generative (forward) models, which differ in respect to the connections (i.e., priors over parameters)
2. Each model is estimated (inverted) using Bayesian model inversion (Variational Bayes), this delivers model evidence and parameter posteriors
3. Competing models can be compared using Bayes Factor and averaged using Averaging (BMA)
4. Having fitted only fully connected DCM models with different priors for each subject, the free energy can be computed using Bayesian Model Reduction (BMR).
5. The models are compared using the Bayes rule for models or the log Bayes factor in the case of equal priors for each model.

DCM pipeline structure and main modules

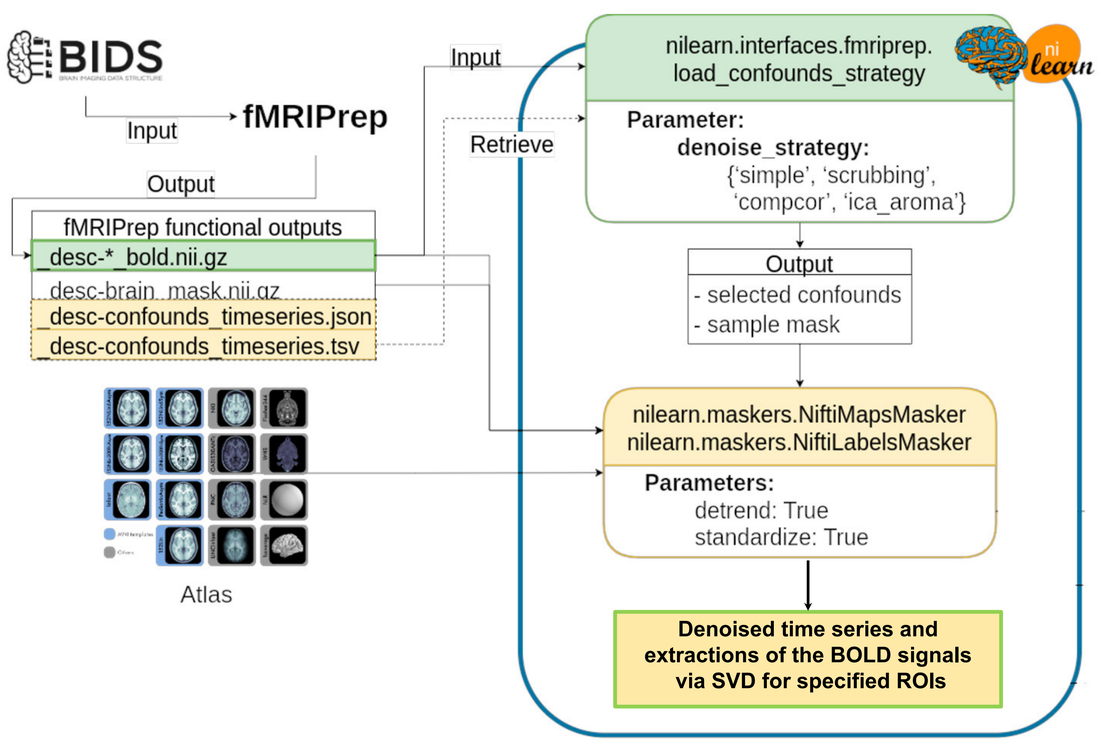

First level analysis: individual DCM models inversion

- Definition of DCM models that are plausible for a specific project and dataset for each subject
- Inversion of the fully connected and predefined DCM models for each subject using MATLAB functions for the spectral DCM in SPM12 Toolbox
- The pipeline output at this level are the individual DCM models for each subject
- The network size appropriate for fitting is limited to 25 nodes

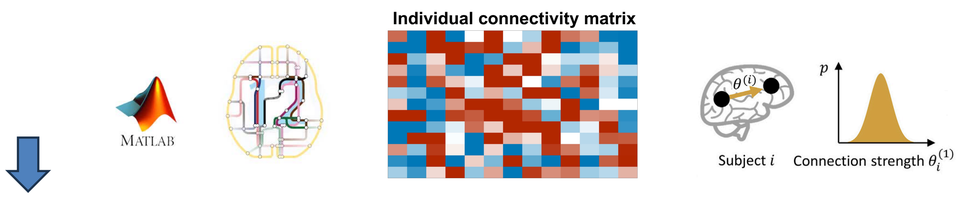

Second level analysis: PEB group analysis

- All individual DCM models were re-fitted using Variational Bayes and empirical priors calculated as group means from the original individual DCMs
- The design matrix specifying confounds and all computed measures is defined
- The pipeline output at this level is the best PEB model, and the BMA posterior estimates at the group level, as well as the commonalities and differences in the case of group comparison
- The network size appropriate for PEB analysis is limited to 20 nodes

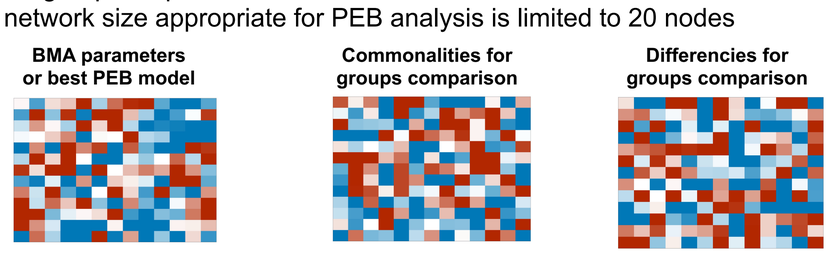

The DCM pipeline is available as git clone https://jugit.fz-uelich.de/a.silchenko/dcm_inm7_alfa.git

DCM pipeline application: Stockholm sleepy brain study dataset

- Stockholm Brain strudy dataset (Karolinska Institute): 41 subjects (age 20-30 years).
- The study was a cross-over comparison between three hours of sleep deprivation (PSD) and full sleep with a one-month interval between measurements [7].
- To study the impact of PSD on intrinsic brain connectivity, we analyzed changes in effective connectivity between the central executive network (CEN), salience network (SN), and the right intraparietal sulcus (rIPS), which is a region densely connected to the frontoparietal networks [8]. The results of the meta-analysis showed that rIPS is hypoactive in total sleep deprivation, but it remains unclear how PSD disrupts its interaction with other networks.
- To reveal changes in the effective connectivity of the rIPS and CEN (13 nodes) and SN (12 nodes) networks, we computed averaged connectivity matrix using BMA over most plausible models, as well as the commonalities (total mean for both groups) and differences (statistically significant deviation from the total mean) in connectivity.
- The obtained matrix with differences in connectivity was modified by excluding connections that were absent before (full sleep state) and after (sleep deprived state) the treatment. The values of the BMA connectivity parameters for the states before and after the treatment were obtained in separate analyses.

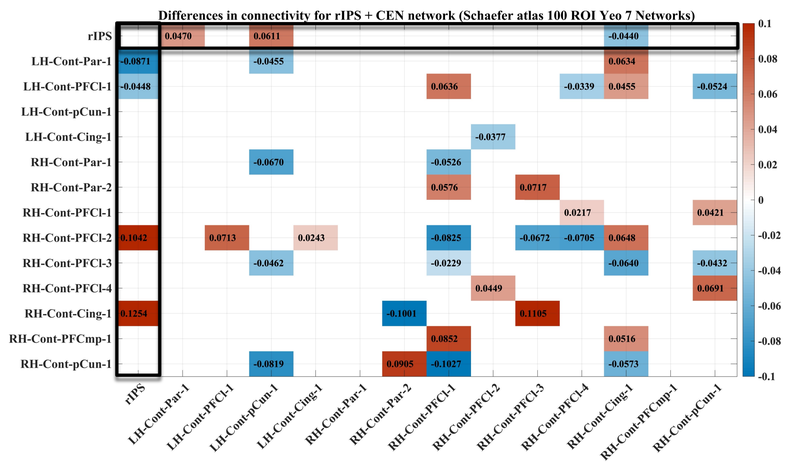

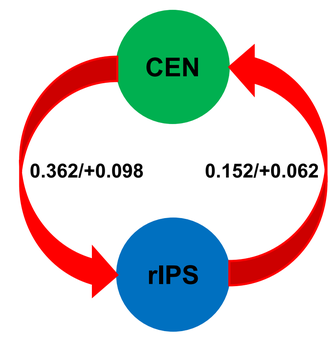

The impact of treatment and changes in rIPS network connectivity and balance were computed as a simple and absolute sum of connection strength changes in the difference matrix (first row and first column)

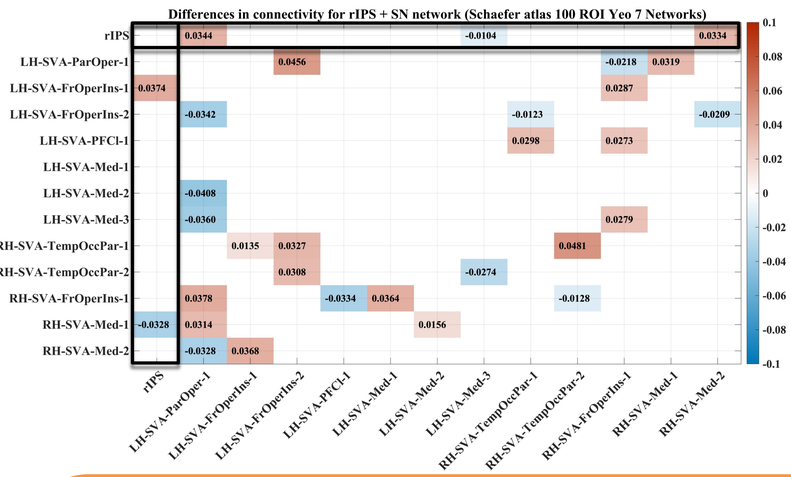

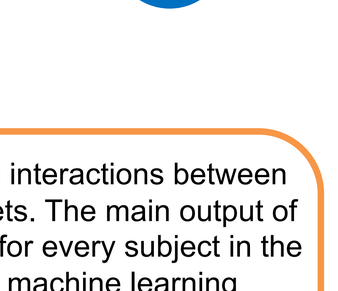

- We developed a computational pipeline to study causal interactions between large-scale brain networks using resting-state fMRI datasets. The main output of the pipeline was the individual connectivity matrices fitted for every subject in the group under study. These matrices can be used in further machine learning studies on directional connectivity between brain regions using large datasets.
- We conducted a comparative analysis of the effective connectivity between large-scale networks before and after three hours partial sleep deprivation using the Stockholm Sleepy brain dataset. Partial sleep deprivation disrupted resting-state effective connectivity between the rIPS, CEN, and SN, enhancing bidirectional interactions between these networks.

References: [1] Friston, K.J., et al. (2003), Neuroimage, vol. 19, pp. 1273-1302; [2] Esteban O., et al. (2019), Nat.Meth. vol. 16, pp. 111-116; [3] Schaefer, A., et al. (2018), Cereb. Cortex, vol. 28, pp. 3095-3114; [4] Razi, A., et al. (2015), Neuroimage, vol. 106, pp. 1-14; [5] Zeidman, P., et al. (2019), Neuroimage, vol. 200, pp. 174-190; [6] Zeidman, P., et al. (2019), Neuroimage, vol. 200, pp. 12-25; [7] Nilsonne G., et al. (2017), Sci. Rep., vol. 7, pp. 9744-9751; [[8] Javaheripour N., et al. (2019), vol. 46, pp. 64-73.

Acknowledgments: This work was supported by the Deutsche Forschungsgemeinschaft (DFG, EI 816/11-1), the National Institute of Mental Health (R01-MH074457), the Helmholtz Portfolio Theme Supercomputing and Modeling for the Human Brain, and the European Union's Horizon 2020 Research and Innovation Programme under Grant Agreements 720270 (HBP SGA1), 785907 (HBP SGA2), and 826421 (VirtualBrainCloud).